Equilibrium Configurations and Energetics of Point Defects in Two-Dimensional Colloidal Crystals

Alexandros Pertsinidis* and X. S. Ling
Department of Physics, Brown University, Providence, Rhode Island 02912
(Received 30 November 2000; published 13 August 2001)

We demonstrate a novel method of introducing point defects (mono- and divacancies) in a confined monolayer colloidal crystal by manipulating individual particles with optical tweezers. Digital video microscopy is used to study defect dynamics in real space and time. We verify the numerical predictions that the stable configurations of the defects have reduced symmetry compared to the triangular lattice and discover that in addition they are characterized by distinct topological arrangements of the particles in the defect core. Surprisingly, point defects are thermally excited into separated dislocations, from which we extract the dislocation pair potential.

DOI: 10.1103/PhysRevLett.87.098303 PACS numbers: 82.70.Dd, 61.72.Bb, 61.72.Ff, 61.72.Ji

Colloidal crystals [1], ordered self-assembled structures of (sub)micron spheres, provide a model system for the study of basic problems in condensed matter physics. In particular, confined colloidal crystals have been used to explore statistical physics in two dimensions [2,3]. Although colloids in 2D have been studied for the last 20 years, several areas still remain relatively unexplored. The simplest structural defects in a crystal, namely vacancies and interstitials, fall in this category. Point defects are of considerable interest, since they play a dominant role in real materials' properties. Also, they are predicted to proliferate in more *exotic* systems, such as the ground state of a Wigner crystal [4] or the supersolid phase [5] of the Abrikosov lattice in type-II superconductors.

Colloidal crystals also offer new approaches in synthesizing materials with novel properties and applications like photonic-band-gap materials [6], optical switches [7], and chemical sensors [8]. Understanding the behavior of defects in colloidal crystals and inventing techniques for manipulating their dynamics can have an immediate impact on the fabrication of nanostructured materials.

In this work we demonstrate the use of optical tweezers [9], a powerful tool that has promoted research in a wide range of fields, to artificially introduce isolated point defects in otherwise structurally perfect two-dimensional colloidal crystals. For the first time, such defects are studied by video microscopy in real space and time, providing new insight into their microscopic dynamics. In this Letter the energetics of the defects are discussed. Results on the diffusion of the defects are presented in a separate publication [10].

The experimental setup is shown in Fig. 1. The colloidal crystals were prepared with a $\approx 1\%$ volume aqueous suspension of 0.360 μm diameter negatively charged polystyrene-sulfate microspheres (Duke Scientific No. 5036, polydispersity $\simeq 1\%$). The suspension was completely deionized by flushing through ion exchange resin [11], and conductivity measurements [12] give an estimated screening length $\kappa^{-1} \approx 390$ nm, originating mainly from the cloud of ≈ 2000 H^+ counterions around each sphere [13,14]. Under these conditions the particles crystallize due to strong electrostatic interaction. Confining the suspension between two fused silica substrates separated by ≈ 2 μm suppresses the vertical motion of the spheres by negative charge that develops at the silica-water interface and creates a single layer colloidal crystal with a lattice constant $a \cong 1.1$ μm [15].

Trapping a particle with optical tweezers and dragging it from its lattice site creates isolated point defects in an otherwise perfect two-dimensional crystal [16]. The optical

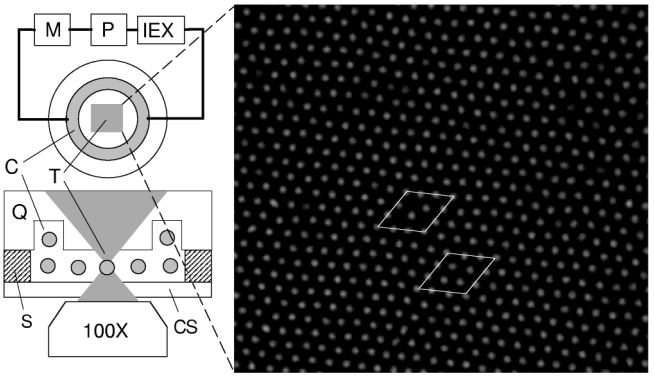

FIG. 1. (Left) Experimental setup (not to scale): The sample cell consists of a 1/2 in. diameter quartz disk (Q) and a quartz coverslip (CS) glued together. The distance between the two surfaces was controlled by a patterned thin (≈ 2 μm) polymer film (S) (Dow Chemical Co., CYCLOTENE), which served both as a spacer and as an adhesive. The cell was connected to an external circulation circuit [11] containing a few ml of suspension, driven by a peristaltic pump (P) (VWR) and including a conductivity meter (M) (VWR, model 1054, flow-through cell) and a column with mixed-bed ion-exchange resin (IEX) [BIO-RAD, AG 501-X8(D)]. (C) Indicates a 0.5 mm circulation channel in contact with the two-dimensional region and (T) a particle trapped with the optical tweezers. (Right) Micrograph of an isolated divacancy in a two-dimensional colloidal crystal. The 4×4 diamond in the enlarged central region contains four particles in the perfect lattice but only two when it encloses the core of the divacancy.

tweezers were formed by focusing a beam of an Ar^+ laser (Coherent INNOVA 90, $\lambda = 514$ nm) through the same objective (Zeiss Plan Neofluar, 100×, oil immersion, NA = 1.3) used for imaging. The position of the beam was controlled by a set of mirrors mounted on an XY galvanometer scanner set (Cambridge Technology). Point defects are created by dragging a particle away from its lattice point at about 50 μm/sec, making it an interstitial and leaving a vacant site behind. To overcome the restoring force from the crystal and to be able to drag the particle faster than the relaxation time of the lattice, 100 mW of laser power (≈50 mW going through the objective lens) was used.

The dynamics of such single, isolated point defects were studied in real time under 100× magnification and recorded on videotape (Sony SVO-9500MD recorder) using a monochrome CCD video-camera (Sony SSC-M370). The field of view covers $(50 \times 40)a^2$. Typically, we processed 60 frames/sec and tracked a single defect for 20–40 sec, which is the time it takes to diffuse away from the field of view. Each individual frame was acquired on a PC and processed using a particle-tracking algorithm [17]. The raw data consists of the positions of the particles in every frame which are linked into trajectories in time.

Real-space imaging facilitates detailed study of the structure of the defect core. The following question naturally arises: what are the possible configurations in which a defect can exist? In the case of strong interactions, $\kappa a \leq 5.9$, where κ^{-1} is the screening length, numerical studies [5,18] of monovacancies and interstitials have revealed that the system spontaneously deforms into configurations with lower symmetry than that of the lattice. This prediction is verified for our system, where $\kappa a \approx 3$ (Figs. 2A–2D). For divacancies, various stable configurations with well defined symmetry can also be identified (Figs. 2E–2H).

The interactions in the system are short ranged [screened Coulomb, $V(r) \propto \exp(-\kappa r)/r$], therefore the nearest neighbor bonds have geometrical as well as physical significance. The creation of a point defect involves the breaking of bonds and creation of miscoordinated particles in the core region. The configuration of the defects can be characterized by the arrangement of these broken bonds and miscoordinated particles. We analyzed the topological structure of the defects by performing a geometrical triangulation of the positions of the particles, finding the pairs of nearest neighbors, and measuring the coordination number n_i for every particle. Our observations indicate that the following constraints are satisfied: (i) the miscoordinated particles are never observed isolated but rather appear as *distinguishable* pairs, triplets, etc., of nearest neighbors, (ii) the mean coordination number of every pair, triplet, etc., is always equal to six, and (iii) we can define vectors $\vec{n}_{ij}$ starting from a particle i with $n_i < 6$ and terminating to a nearest neighbor j with $n_j > 6$. The number of vectors originating from i is $6 - n_i$ and the number of vectors terminating on j is $n_j - 6$. For every configuration, $\sum_{\langle ij \rangle} \vec{n}_{ij} \approx 0$.

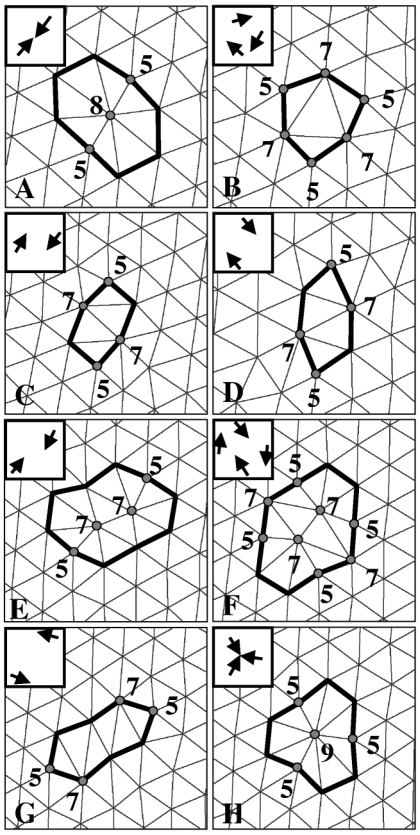

FIG. 2. Configurations of monovacancy: (A) split (SV), (B) threefold symmetric (V_3), (C),(D) twofold crushed (V_{2a}, V_{2b}). Nomenclature adopted from [18]. Top left insets in every figure show configuration of the vectors $\vec{n}_{ij}$ defined in the text. The grey dots show the arrangement of miscoordinated particles in the core of the defect. The relative free energies of the different configurations were estimated to be (in k_BT): $F_{SV} = 0.86$, $F_{V3} = 1.10$, $F_{V_{2a}+V_{2b}} = 1.41$. Configurations of divacancy: (E),(F) split ($SD_{a,b}$), (G) twofold crushed (D_2), (H) threefold symmetric (D_3). Free energies in k_BT are $F_{D2} = 0.7$, $F_{SD_a+SD_b} = 1.1$, and $F_{D3} = 2.1$.

The finite temperature causes the system to vibrate around every local energy minimum C, exploring the volume of phase space Ω_C in which the energy is $O(k_BT)$ above the minimum energy E_C, and occasionally getting enough energy to jump to a nearby local minimum. The contribution to the entropy of every configuration is roughly $S_C = k \log(\Omega_C)$, and the different configurations occur with relative probabilities $P_C \propto \exp(-F_C/k_BT)$, where $F_C = E_C - TS_C$ is the *free* energy of a configuration. As long as the system remains around a local energy minimum, the distortions of the lattice are elastic and the topological arrangement of the particles does not change. Therefore, every energy minimum has not only a characteristic symmetry but also a certain topological configuration of the defect core. Using the topology rather than the symmetry as a criterion for identifying the different configurations C, we measure their relative occurrence probabilities P_C. The free energy differences, estimated from the measured P_C's, are found to be of order 0.1–1 k_BT.

Point defects are "topologically neutral" since they have zero Burgers vector. However, one could think of creating a point defect by inserting extra rows of particles that do not terminate on each other. The extra inserted rows are edge dislocations whose Burgers vectors add up to zero. Therefore, a point defect contains embryonic pairs, triplets, etc., of dislocations, in the same way that a dislocation contains an embryonic pair of a sevenfold and a fivefold disclination [19]. Since the system is at finite temperature, one would expect the defect to fluctuate between these possible configurations of dislocations.

The signature of an isolated edge dislocation in a two-dimensional hexagonal lattice is a core with a pair of neighbor fivefold and sevenfold coordinated particles. The extra row of particles terminates on the fivefold particle. The Burgers vector $\vec{b} = \vec{a}$ is in one-to-one correspondence with the vector $\vec{n}_{ij}$ defined earlier in the text. $\vec{b}$ connects the fivefold coordinated particle with its first nearest neighbor, moving counterclockwise after the sevenfold neighbor (see Fig. 3). Since $\vec{b} \leftrightarrow \vec{n}_{ij}$ and $\sum_{\langle ij \rangle} \vec{n}_{ij} \approx 0$, one can view the various configurations of the defect as $\sum \vec{b} = 0$ *dislocation multipoles.* Tracking the time evolution of the system, we see that the vast majority of the observed configurations correspond to a dislocation pair or a triplet, with infrequent appearance of higher order multipoles. Most of the time the dislocations comprising the defect are closely bound in the configurations previously identified (Fig. 2). Occasionally, however, configurations are observed in which the dislocations appear to dissociate and recombine (Fig. 3). This fits well with a picture in which the dislocations are considered point particles with opposite topological charge (Burgers vector) interacting with an attractive potential.

Focusing on the case in which the point defects appear as a dislocation pair and assuming an interaction $V(\vec{r})$ between the two dislocations, we would expect Boltzmann statistics for the probability of observing the two dislocations a certain distance apart, namely, $P(\vec{r}) \propto \exp[-V(\vec{r})/k_BT]$. In addition, particle conservation dictates that dislocations can only glide parallel to their Burgers vector, so $\vec{r} = \vec{r}_c + \vec{r}_g$, with $\vec{r}_c \approx 3\vec{a}(2\vec{a})$ for di(mono)vacancy and $\vec{r}_g \parallel \vec{b}$. We measured $P(r)$, $r = |\vec{r}|$, for the mono- and divacancies, using a few thousand snapshots of the system. The separation r of the two dislocations is identified as the separation between the two fivefold coordinated particles where the extra rows of particles terminate. Our results (Fig. 4) show a rather rapid decrease in $P(r)$ as r goes beyond a couple of lattice constants, together with a modulation, more clearly seen in the case of the divacancy. Since $V(r) \propto -\log P(r)$, the interaction of the two dislocations turns out to increase with r, with an average slope $(2.9 \pm 0.4)k_BT/a$ and $(2.0 \pm 0.2)k_BT/a$ for the case of mono- and divacancy, respectively. The modulation is due to a Peierls energy barrier [20] that comes from the discreteness of the lattice. A final point is that the core region of dislocations has a typical size of a few a. Therefore, our measurements of $V(r)$ are in a regime where the cores of the two dislocations overlap and linear elasticity theory is not applicable.

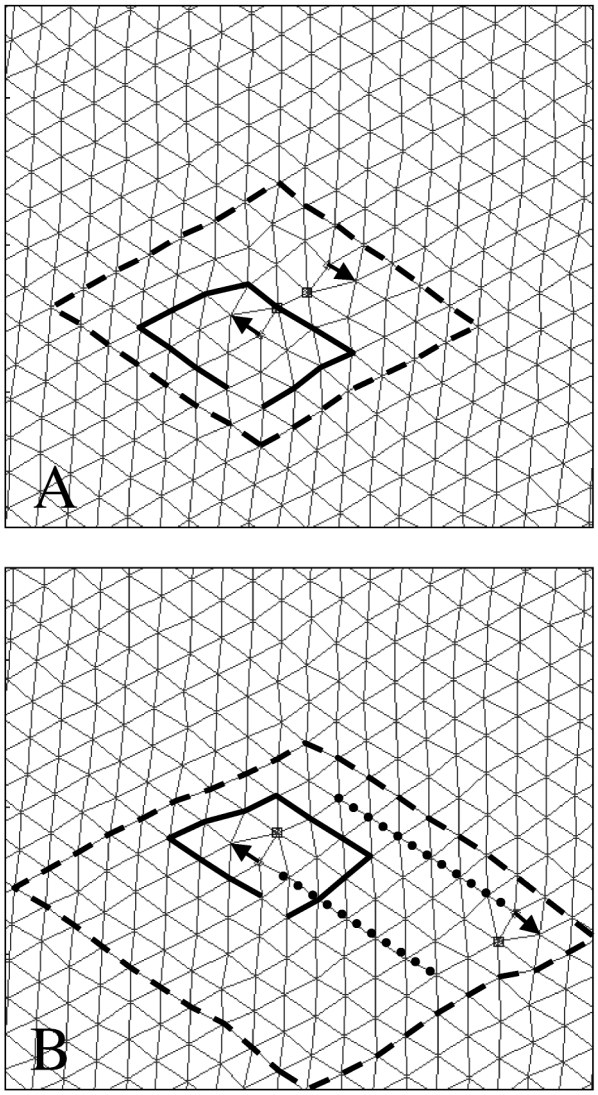

FIG. 3. Point defects as dislocation multipoles: (A) Well-defined divacancy configuration. A Burgers circuit (solid line) fails to close if it crosses the core of the defect. A Burgers circuit that surrounds the defect core without crossing it (dashed line) closes as expected. The arrows indicate the Burgers vectors of the "embryonic" dislocation dipole. (B) Configuration of the same divacancy about 2 sec later. The divacancy is not well defined any more and the system resembles a pair of dislocations with opposite Burgers vectors, whose gliding lines (dotted lines) are separated by $\approx 3\vec{a}$. When those two dislocations come close to each other, the original divacancy is recovered.

In summary, we have demonstrated a novel way of introducing point defects in colloidal crystals through manipulation of individual particles with optical tweezers. Using digital video microscopy, we observed that the stable configurations of the defects have reduced symmetry compared to the triangular lattice and identified distinct topological features in the arrangement of the system in every configuration. This analysis demonstrates that topologically the point defects correspond to dislocation *multipoles* with zero total Burgers vector. The individual dislocations

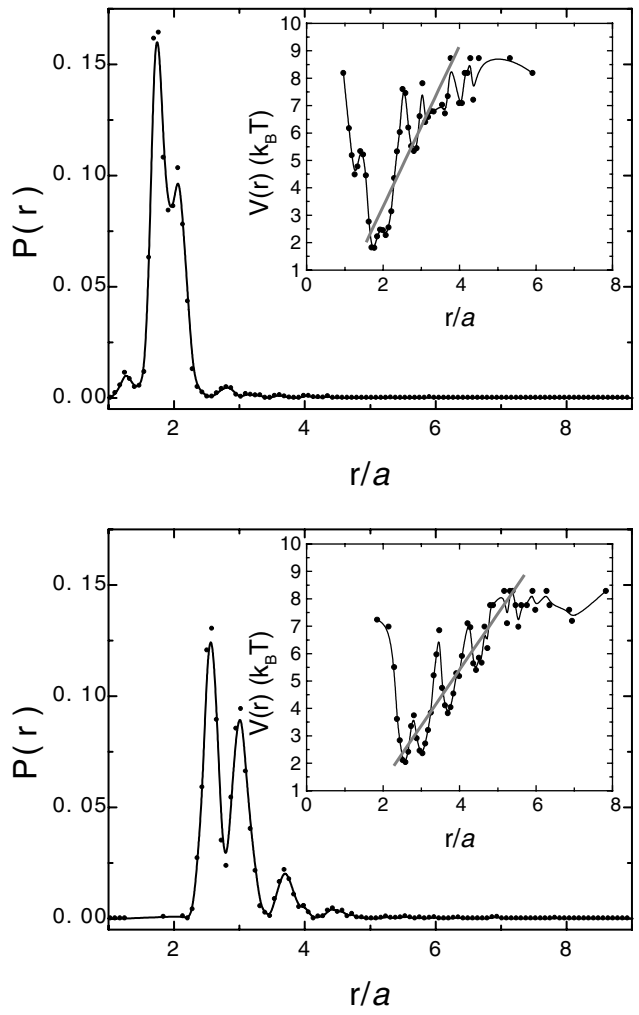

FIG. 4. Pair interaction between dislocations, divacancies (top) and monovacancies (bottom). $P(r)$ was determined from a few thousand snapshots of the system by measuring the distribution of the separation of the two fivefold coordinated particles found. Insets: $V(r)/k_BT$ was estimated from $-\log P(r)$. The solid curves are spline fits and the straight lines are linear fits to the particular regions of data.

are bound by an attractive interaction. Divacancies in particular are observed to dissociate into two dislocations that can separate several lattice spacings before recombination.

We acknowledge helpful discussions with Professor D. G. Grier and Professor S. C. Ying. This work was supported by NSF (Grant No. DMR-9804083), the Petroleum Research Fund, and the Research Corporation. X. S. L. acknowledges the support of the A. P. Sloan Foundation.

*Email address: pertsin@barus.physics.brown.edu

[1] A. P. Gast and W. B. Russel, Phys. Today **51**, No. 12, 24 (1998).

[2] C. A. Murray, in *Bond-orientational Order in Condensed Matter Systems,* edited by K. J. Strandburg (Springer, New York, 1992).

[3] K. Zahn, R. Lenke, and G. Maret, Phys. Rev. Lett. **82**, 2721 (1999).

[4] D. S. Fisher, B. I. Halperin, and R. Morf, Phys. Rev. B **20**, 4692 (1979).

[5] E. Frey, D. R. Nelson, and D. S. Fisher, Phys. Rev. B **49**, 9723 (1994).

[6] J. E. G. J. Wijnhoven and W. L. Vos, Science **281**, 802 (1998).

[7] G. Pan, R. Kesavamoorthy, and S. A. Asher, Phys. Rev. Lett. **78**, 3860 (1997).

[8] J. H. Holtz and S. A. Asher, Nature (London) **389**, 829 (1997).

[9] A. Ashkin, J. M. Dziedzic, J. E. Bjorkholm, and S. Chu, Opt. Lett. **11**, 288 (1986).

[10] A. Pertsinidis and X. S. Ling, Nature (London) (to be published).

[11] T. Palberg, W. Härtl, U. Wittig, H. Versmold, M. Würth, and E. Simnacher, J. Phys. Chem. **96**, 8180 (1992); R. Biehl and T. Palberg, Prog. Colloid Polym. Sci. **115**, 300 (2000).

[12] T. Palberg, M. Evers, N. Garbow, and D. Hessinger, in *Transport and Structure: Their Competitive Roles in Biophysics and Chemistry,* edited by S. C. Müller, J. Parisi, and W. Zimmermann (Springer, Berlin, Heidelberg, 1999); D. Hessinger, M. Evers, and T. Palberg, Phys. Rev. E **61**, 5493 (2000).

[13] S. Alexander *et al.,* J. Chem. Phys. **80**, 5776 (1984).

[14] The conductivity of the suspension is given by $\sigma = \rho Z^* e(\mu_P + \mu_{H^+}) + \sigma_{H_2O} + \sigma_B$, where ρ is the concentration of colloidal particles, Z^*e is the effective particle charge, μ_P is the particle mobility, and $\mu_{H^+} = 3.62 \times 10^{-7}\ \mathrm{V\,m^{-1}\,s^{-1}}$ is the proton mobility [12]. The contributions $\sigma_{H_2O} = 0.055\ \mu\mathrm{S\,cm^{-1}}$ and σ_B from water and background stray ions (concentration $\sim 10^{-7}$ M) can be neglected. The particles do not contribute more than a few percent due to their small mobility $\mu_P \sim 10^{-8}\ \mathrm{V\,m^{-1}\,s^{-1}}$. Since the suspension is completely deionized, the screening of the particles' charge comes from the H^+ counterions, therefore $\kappa^2 = 4\pi\lambda_B\rho Z^*$, where $\lambda_B = 0.715$ nm is the Bjerrum length [13]. Measurement of σ directly gives an estimate for the screening length: $\kappa^2 = 4\pi\lambda_B\sigma/(e\mu_{H^+})$, or $\kappa^{-1} \approx 634/\sqrt{\sigma}$ nm, with σ given in $\mu\mathrm{S\,cm^{-1}}$. For the 1% volume suspension used in our studies, $\sigma = 2.5\ \mu\mathrm{S\,cm^{-1}}$ resulting in $Z^* = 1650$ and $\kappa^{-1} \approx 390$ nm.

[15] The two-dimensional region extended over a few hundred lattice constants. We used optical tweezers to drag impurities, such as aggregates of particles, away from a central region 40×40 lattice constants, where the experiments were performed. In these experimental conditions (density of particles and screening length) the resulting two-dimensional crystal was deep in the solid phase, with no thermally generated defects.

[16] Video clips can be found at the following URL: http://www.physics.brown.edu/Users/students/pertsinidis/Research.html.

[17] J. C. Crocker and D. G. Grier, J. Colloid Interface Sci. **179**, 298 (1996).

[18] S. Jain and D. R. Nelson, Phys. Rev. E **61**, 1599 (2000).

[19] This picture is utilized in the theory of melting in 2D; see D. R. Nelson, in *Phase Transitions and Critical Phenomena,* edited by C. Domb and J. Lebowitz (Academic, London, 1983), Vol. 7, Chap. 1.

[20] F. R. N. Nabarro, *Theory of Crystal Dislocations* (Dover, New York, 1987), Chap. 3.